ACS APPLIED MATERIALS & INTERFACES

Letter

www.acsami.org

Novel BODIPY-Based Fluorescence Turn-on Sensor for Fe^{3+} and Its Bioimaging Application in Living Cells

Binglin Sui,[†] Simon Tang,[†] Taihong Liu,[†] Bosung Kim,[†] and Kevin D. Belfield*[,†,‡,§]

[†]Department of Chemistry and [‡]CREOL, The College of Optics and Photonics, University of Central Florida, Orlando, Florida 32816, United States

[§]School of Chemistry and Chemical Engineering, Shaanxi Normal University, Xi'an, 710062, P.R. China

Supporting Information

ABSTRACT: A novel boron-dipyrromethene (BODIPY) based fluorescence turn-on sensor for detecting Fe^{3+} in aqueous media is reported with 23-fold fluorescence enhancement. The sensor is comprised of a combination of BODIPY fluorophore and a new Fe^{3+}-recognizing cryptand that exhibits high selectivity, sensitivity, and reversibility toward Fe^{3+} detection. Cell imaging studies demonstrate that this sensor is capable of sensing Fe^{3+} in living cells.

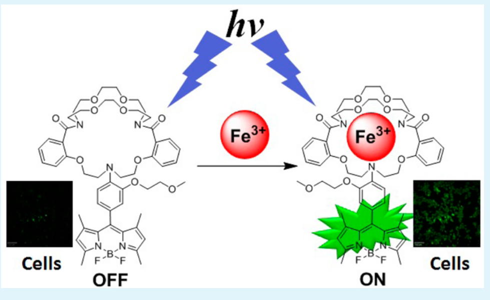

KEYWORDS: *iron(III), fluorescent sensor, BODIPY, cryptand, cell imaging, metal ion sensor*

With the recognition of the importance of various transition metal ions in a wide range of environmental and biological processes, the development of sensors for transition metal ion detection has attracted a great deal of attention over the past two decades. Among all the transition metals, iron, the physiologically most abundant and versatile transition metal in biological systems, is no doubt one of the most important because of the crucial roles it plays in oxygen uptake, oxygen metabolism, electron transfer, and transcriptional regulation.[1−5] On the other hand, excessive Fe^{3+} ions within the body have been associated with the development of severe diseases including various cancers, hepatitis, hemochromatosis, and dysfunction of organs, such as the liver, heart, and pancreas.[6−8] Moreover, recent research has revealed that Fe^{3+} is also involved in neurodegenerative diseases, such as Alzheimer's disease and Parkinson's disease.[9−11] Therefore, intense research efforts have been devoted to the development of chemosensors for Fe^{3+} ion detection.[12]

Compared to other techniques, fluorescence methods have a number of advantages such as high sensitivity, noninvasiveness, and convenience. As a result, a number of fluorescent chemosensors have been developed for probing the Fe^{3+} ion.[13−23] However, most of these fluorescent Fe^{3+} sensors are based on fluorescence quenching mechanisms, which limits their application in biological systems.[16−19] In recent years, rhodamine-based fluorescence turn-on probes for Fe^{3+} ion detection have been reported.[20−23] The "off-on" fluorescence changes exhibited by these dyes are generated from Fe^{3+}-induced transformation from the spirocyclic form to the ring-opened form of the rhodamine system.[13] These sensors are generally irreversible because of their reaction-based nature.

Herein, we present a novel, reversible fluorescence turn-on sensor for Fe^{3+} ion determination in aqueous media. The sensor (**1**) is composed of two moieties, a BODIPY (4,4-difluoro-4−3a, 4a-diaza-s-indacene) platform as the fluorophore and a 1,10-diaza-18-crown-6 based cryptand as the Fe^{3+} recognition unit. The synthesis of sensor **1** started from 2-(2-methoxyethoxy)aniline and 1,10-diaza-18-crown-6 (Scheme 1). The bis(hydroxyethyl)aniline derivative **2**, prepared according to the literature,[24] was formylated via a Vilsmeier−Haack reaction to produce aldehyde **3** while the hydroxyl groups were converted to chloro groups by $POCl_3$. Cryptand **4** was obtained via reaction of 1,10-diaza-18-crown-6 and *o*-acetylsalicyloyl chloride in the presence of triethylamine (TEA). Removal of the acetyl groups of **4** afforded cryptand **5**. Tricyclic cryptand **6** was synthesized through a macrocyclization reaction between aldehyde **3** and bicyclic cryptand **5** in highly dilute DMF solution. Trifluoroacetic acid (TFA)-catalyzed condensation reaction of **6** with 2,4-dimethylpyrrole provided the target sensor **1** in 13% yield.

UV−vis absorption measurements of **1** were carried out in a H_2O-CH_3CN (9:1 v/v) solution. The free sensor **1** showed an absorption peak at 499 nm (see Figure S1 in the Supporting Information). The addition of Fe^{3+} resulted in a decrease in the absorption intensity of **1**. In addition to Fe^{3+}, Cr^{3+} also brought about a reduction in the absorption maximum of **1**, which was much weaker of an effect than that induced by Fe^{3+}. The addition of Hg^{2+} generated a slight decrease in the absorption intensity and a small bathochromic shift in the absorption

Received: July 14, 2014
Accepted: October 20, 2014
Published: October 22, 2014

Scheme 1. Synthetic Route for Sensor 1[a]

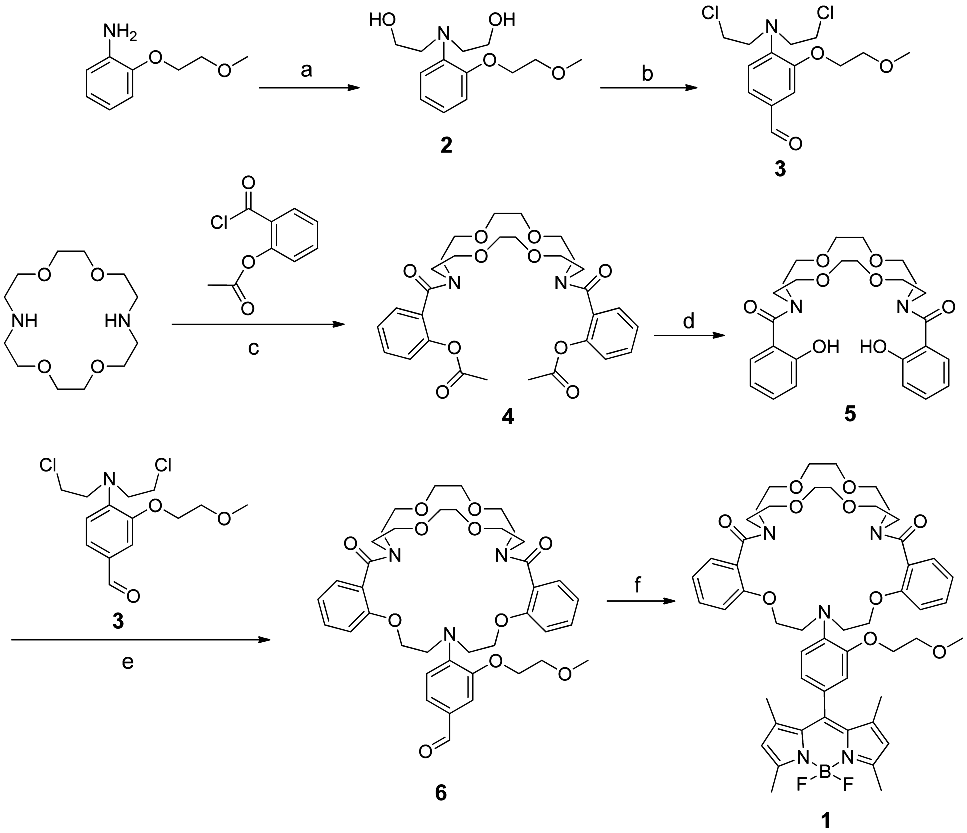

[a]Reagents and conditions: (a) 2-chloroethanol, $CaCO_3$, KI, H_2O, reflux, overnight; (b) DMF, $POCl_3$, 0 to 60 °C, overnight; (c) TEA, CH_2Cl_2, room temperature, 2 h; (d) $NaHCO_3$, NH_4OAc, aqueous CH_3OH (1:1), reflux, overnight; (e) KI, Cs_2CO_3, DMF, 105 °C, 6 d; (f) 2,4-dimethylpyrrole, TFA, CH_2Cl_2, room temperature, overnight; then DDQ, 4 h; then TEA, $BF_3{\cdot}OEt_2$, overnight.

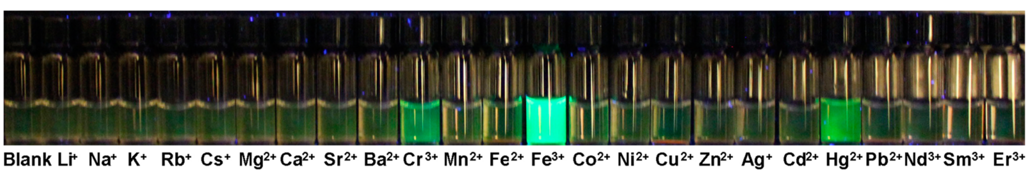

Figure 1. Visual fluorescence responses of **1** (7 μM) in H_2O−CH_3CN (9:1, v/v) upon addition of 100 equiv of various metal cations with excitation at 365 nm using a hand-held UV lamp.

maximum. No considerable change was observed upon the addition of other metal cations of interest, including Li^+, Na^+, K^+, Rb^+, Cs^+, Mg^{2+}, Ca^{2+}, Sr^{2+}, Ba^{2+}, Mn^{2+}, Fe^{2+}, Co^{2+}, Ni^{2+}, Cu^{2+}, Zn^{2+}, Ag^+, Cd^{2+}, Pb^{2+}, Nd^{3+}, Sm^{3+}, and Er^{3+}. These results demonstrate that sensor **1** is quite selective in detecting Fe^{3+}. Moreover, as shown in Figure S2 in the Supporting Information, the absorption intensity of **1** decreased gradually upon the addition of the first 4 equiv of Fe^{3+}. After that, subsequent addition of additional Fe^{3+} brought about no further change in the absorption spectra of sensor **1**.

Compared to UV−vis spectroscopy, fluorescence emission spectroscopy is a more effective technique for Fe^{3+} ion detection due to its high sensitivity. The selectivity of **1** as a Fe^{3+} sensor was thus investigated through fluorescence emission spectroscopy by adding the afforementioned metal cations to a H_2O−CH_3CN (9:1 v/v) solution of sensor **1**. Figure 1 illustrates the visual fluorescence response of sensor **1** with excitation at 365 nm using a hand-held UV lamp. In the absence of metal cations, the free sensor **1** displayed very weak fluorescence, whereas a striking yellow-green fluorescence, characteristic of BODIPY derivatives, with a maximum wavelength at 512 nm emerged quickly after Fe^{3+} was introduced to the solution of **1**. Weaker fluorescence responses of sensor **1** were induced by the addition of Cr^{3+} and Hg^{2+} ions, and no apparent fluorescence change was observed upon adding other metal cations of interest. Detailed changes in the fluorescence emission spectra of **1**, triggered by various metal cations, are demonstrated in Figure S3 in the Supporting Information. The excitation wavelength was 480 nm. In the presence of 100 equiv of Fe^{3+}, a prominent enhancement of fluorescence emission (28-fold) for sensor **1** solution was observed. However, very modest fluorescence increases were observed for the addition of 100 equiv of Cr^{3+} (4-fold) and Hg^{2+} (3-fold). In addition to a slight increase in the fluorescence emission intensity of **1** upon the addition of Hg^{2+} ions, a small bathochromic shift in the maximum fluorescence emission wavelength occurred (from 512 to 522 nm), consistent with the UV−vis absorption measurements

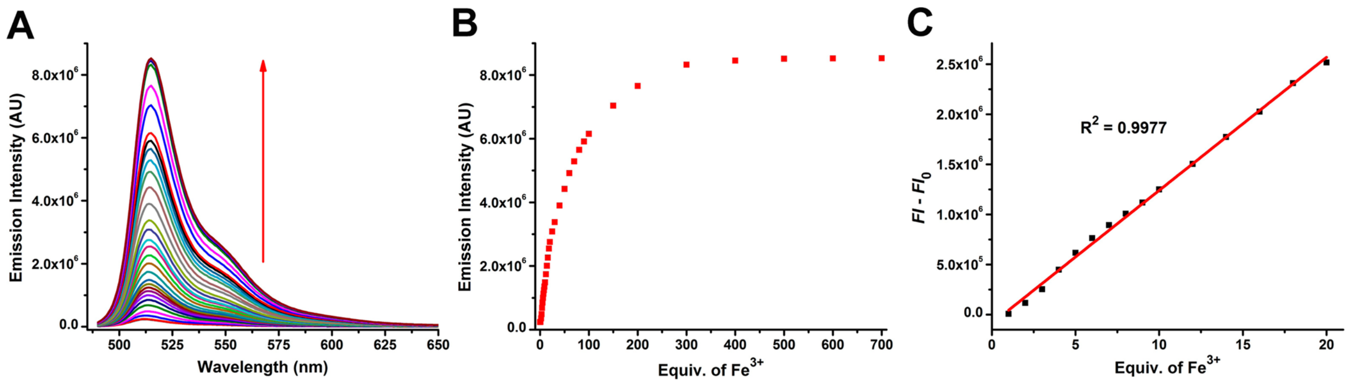

Figure 2. (A) Enhancements in fluorescence emission of sensor **1** (7 μM) in H_2O-CH_3CN (9:1 v/v) upon continuous addition of 1−700 equiv of Fe^{3+} ions. (B) Fluorescence emission intensity of **1** as a function of the equiv of added Fe^{3+}. (C) Plot of FI − FI_0 (FI: fluorescence intensity) versus the equiv of Fe^{3+} added in the range of 1−20 equiv of Fe^{3+} ions. λ_{ex} = 480 nm.

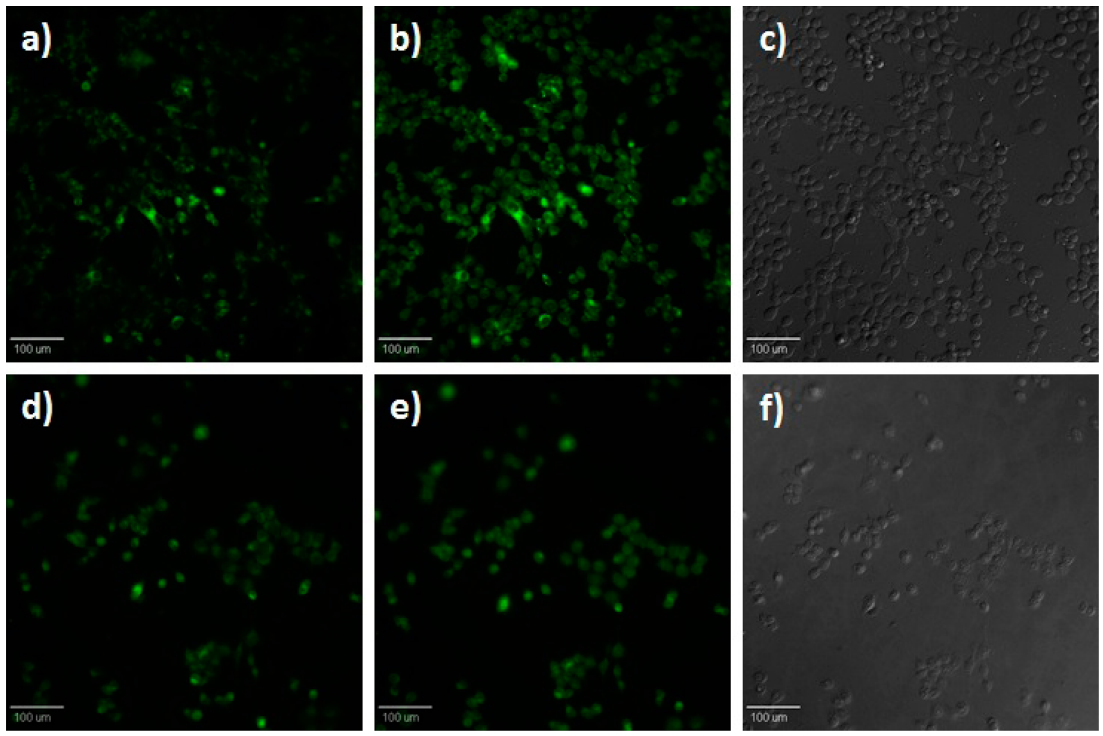

Figure 3. Images of live HCT-116 cells (a−c) in the presence of 30 μM Fe^{3+} solution in MEM medium and (d−f) without Fe^{3+} in only MEM medium at (a, d) 0 and (b, e) 60 min after incubation with sensor **1** (20 μM). c and f are the phase contrast images of b and e, respectively.

described above. Upon the addition of 100 equiv of other metal ions, little to no change in fluorescence emission of **1** was detected. These results support the high selectivity of sensor **1** to Fe^{3+}. Sensor **1** was designed on the basis of a PET (photoinduced electron transfer) mechanism that has been widely used to develop fluorescence turn-on probes for various metal cations.[25] Upon binding to Fe^{3+}, the PET process from the cryptand to the BODIPY fluorophore is inhibited, resulting in strongly enhanced fluorescence emission.

To further investigate the efficiency of sensor **1** toward Fe^{3+} detection, we carried out fluorescence emission titration experiments. As shown in Figure 2A, a gradual enhancement of the fluorescence intensity of sensor **1** was observed upon progressive addition of Fe^{3+} ion. According to the Benesi−Hildebrand equation,[26] the K_d value of the sensor was determined to be 1.0×10^{-4} M. The detailed relationship between the fluorescence intensity of **1** and the equiv of Fe^{3+} ion added is illustrated in Figure 2B. The addition of an initial 20 equiv of Fe^{3+} led to a dramatic increase of the fluorescence emission of sensor **1**. After that, the increase in Fe^{3+}-induced fluorescence enhancement slowed down following titration of up to 300 equiv of Fe^{3+}, then the fluorescence emission generally stabilized. More significantly, as exhibited in Figure 2C, the plot of the fluorescence intensity enhancement (FI − FI_0, FI: fluorescence intensity) versus equiv of Fe^{3+} was found to be linear (R^2 = 0.9977) in the range of 1−20 equiv of Fe^{3+} ions. The detection limit of sensor **1** for Fe^{3+} was determined to be 1.3×10^{-7} M. Therefore, sensor **1** has potential for quantitative determination of the concentration of Fe^{3+}.

To further study the interaction between sensor **1** and Fe^{3+}, the reversibility of sensor **1** for Fe^{3+} sensing was investigated (see Figure S4 in the Supporting Information). As expected, when 20 equiv of Fe^{3+} was added to a H_2O-CH_3CN (9:1 v/v) solution of sensor **1**, a noticeable fluorescence emission

dx.doi.org/10.1021/am506262u | ACS Appl. Mater. Interfaces 2014, 6, 18408−18412

enhancement was recorded. Subsequently, N,N,N′,N′-tetrakis-(2-pyridylmethyl)ethylenediamine) (TPEN), a strong Fe^{3+} chelator, was added to the solution and an apparent fluorescence decrease was instantly observed. The fluorescence emission spectrum of sensor **1** in the presence of 20 equiv of Fe^{3+} ions was recovered back to the original spectrum of free sensor **1** upon the addition of 60 equiv of TPEN (3 equiv. for Fe^{3+}). These results suggest that the sensing ability of sensor **1** for Fe^{3+} ion is reversible.

In addition, the pH sensitivity of sensor **1** was also examined in H_2O-MeCN (9:1, v/v) solutions at different pH values between 2.0 and 9.0. As displayed in Figure S5 in the Supporting Information, no apparent change of the fluorescence emission spectra of sensor **1** was detected in the pH range of 3.2−9.0. When the pH of the sample was reduced to 3.0, enhancement in the fluorescence intensity of sensor **1** was observed. These results indicate that sensor **1** is pH insensitive in the physiological pH range (6.8−7.4).

Sensor **1** was also explored to detect Fe^{3+} in living cells. Cell viability tests with HCT-116 cells showed no level of toxicity for varying concentrations of sensor **1** up to 25 μM (see Figure S6 in the Supporting Information). Cell imaging experiments were conducted to investigate the Fe^{3+} sensing ability of probe **1** in living cells. Figure 3 shows the fluorescence images and phase contrast images of cells, whereas the average fluorescence emission intensity of cells at different times is shown in Figure S7 in the Supporting Information. HCT-116 cells were incubated with a 20 μM solution of sensor **1** in MEM medium for 10 min. Then a 30 μM Fe^{3+} solution in MEM medium was pumped into the cell chambers and cells were imaged immediately (Figure 3a). For the control experiment, only MEM medium was used instead of the Fe^{3+} solution (Figure 3d). Cell images were then recorded every 10 min. After 60 min, a significant increase in fluorescence was observed for the cells incubated with Fe^{3+} solution (Figure 3b), whereas no obvious change could be found for cells treated with only MEM medium (Figure 3e). Fluorescence intensity data of cells at different time points quantitatively demonstrated the fluorescence signal change of cells (see Figure S7 in the Supporting Information). Cells incubated with Fe^{3+} solution displayed gradually increased fluorescence with incubation time (curve B in Figure S7 in the Supporting Information). In contrast, fluorescence from cells without Fe^{3+} incubation remained fairly constant (curve A in Figure S7 in the Supporting Information). In addition, the phase contrast images (Figure 3c, f) showed that those cells were still in good condition (viable). These results indicate that sensor **1** is capable of sensing Fe^{3+} in living cells without causing noticeable damage to cells.

In summary, a novel BODIPY-based selective, sensitive, and reversible fluorescence turn-on sensor (**1**) for Fe^{3+} ion detection was synthesized and characterized. Sensor **1** is a conjugate of two moieties, a BODIPY platform serving as the fluorophore and a 1,10-diaza-18-crown-6 based cryptand acting as the Fe^{3+} recognition element. Sensor **1** exhibited very good selective fluorescence turn-on response toward Fe^{3+} ions over other metal cations of interest, including Cr^{3+} and Hg^{2+} ions, which are the most common interfering metal ions for Fe^{3+} detection. Also, sensor **1** demonstrated high sensitivity for Fe^{3+} sensing with a linear relationship observed between the fluorescence intensity enhancement and the equiv of added Fe^{3+} ion. Moreover, the turn-on fluorescence response of sensor **1** to Fe^{3+} ions was reversible; treatment of Fe^{3+}-loaded sensor **1** with TPEN restored the fluorescence emission back to baseline levels. On the basis of its excellent performance in Fe^{3+} sensing and very low cytotoxicity, sensor **1** was successfully applied to detect Fe^{3+} in living cells.

■ ASSOCIATED CONTENT

Supporting Information

Information on the synthesis and corresponding characterization data for compounds **1−6**, absorption spectra, cell culture for imaging, cytotoxicity of sensor **1**, fluorescence intensity of cell images, and ^{1}H and ^{13}C spectra. This material is available free of charge via the Internet at http://pubs.acs.org.

■ AUTHOR INFORMATION

Corresponding Author

*E-mail: Belfield@ucf.edu.

Notes

The authors declare no competing financial interest.

■ ACKNOWLEDGMENTS

We acknowledge the National Science Foundation (CHE-0832622) and the U.S. National Academy of Sciences (PGA-P210877).

■ REFERENCES

(1) Beutler, E. ″Pumping″ Iron: The Proteins. *Science* **2004**, *306*, 2051−2053.

(2) Dai, S.; Schwendtmayer, C.; Schürmann, P.; Ramaswamy, S.; Eklund, H. Redox Signaling in Chloroplasts: Cleavage of Disulfides by an Iron-Sulfur Cluster. *Science* **2000**, *287*, 655−658.

(3) Atkinson, A.; Winge, D. R. Metal Acquisition and Availability in the Mitochondria. *Chem. Rev.* **2009**, *109*, 4708−4721.

(4) Kaplan, C. D.; Kaplan, J. Iron Acquisition and Transcriptional Regulation. *Chem. Rev.* **2009**, *109*, 4536−4552.

(5) Theil, E. C.; Goss, D. J. Living with Iron (and Oxygen): Questions and Answers About Iron Homeostasis. *Chem. Rev.* **2009**, *109*, 4568−4579.

(6) Galaris, D.; Skiada, V.; Barbouti, A. Redox Signaling and Cancer: The Role of ″Labile″ Iron. *Cancer Lett.* **2008**, *266*, 21−29.

(7) Weinberg, E. D. The Role of Iron in Cancer. *Eur. J. Cancer Prev.* **1996**, *5*, 19−36.

(8) Halliwell, B. Reactive Oxygen Species and the Central Nervous System. *J. Neurochem.* **1992**, *59*, 1609−1623.

(9) Dornelles, A.; Garcia, V.; Lima, M. M.; Vedana, G.; Alcalde, L.; Bogo, M.; Schröder, N. Mrna Expression of Proteins Involved in Iron Homeostasis in Brain Regions Is Altered by Age and by Iron Overloading in the Neonatal Period. *Neurochem. Res.* **2010**, *35*, 564−571.

(10) Gaeta, A.; Hider, R. C. The Crucial Role of Metal Ions in Neurodegeneration: The Basis for a Promising Therapeutic Strategy. *Br. J. Pharmacol.* **2005**, *146*, 1041−1059.

(11) Molina-Holgado, F.; Hider, R.; Gaeta, A.; Williams, R.; Francis, P. Metals Ions and Neurodegeneration. *Biometals* **2007**, *20*, 639−654.

(12) McRae, R.; Bagchi, P.; Sumalekshmy, S.; Fahrni, C. J. In Situ Imaging of Metals in Cells and Tissues. *Chem. Rev.* **2009**, *109*, 4780−4827.

(13) Kim, H. N.; Lee, M. H.; Kim, H. J.; Kim, J. S.; Yoon, J. A New Trend in Rhodamine-Based Chemosensors: Application of Spirolactam Ring-Opening to Sensing Ions. *Chem. Soc. Rev.* **2008**, *37*, 1465−1472.

(14) Qu, X.; Liu, Q.; Ji, X.; Chen, H.; Zhou, Z.; Shen, Z. Enhancing the Stokes' Shift of Bodipy Dyes Via through-Bond Energy Transfer and Its Application for Fe^{3+}-Detection in Live Cell Imaging. *Chem. Commun.* **2012**, *48*, 4600−4602.

(15) Sahoo, S. K.; Sharma, D.; Bera, R. K.; Crisponi, G.; Callan, J. F. Iron(III) Selective Molecular and Supramolecular Fluorescent Probes. *Chem. Soc. Rev.* **2012**, *41*, 7195−7227.

(16) Bodenant, B.; Fages, F.; Delville, M.-H. Metal-Induced Self-Assembly of a Pyrene-Tethered Hydroxamate Ligand for the Generation of Multichromophoric Supramolecular Systems. The Pyrene Excimer as Switch for Iron(III)-Driven Intramolecular Fluorescence Quenching. *J. Am. Chem. Soc.* **1998**, *120*, 7511−7519.
(17) Fakih, S.; Podinovskaia, M.; Kong, X.; Schaible, U. E.; Collins, H. L.; Hider, R. C. Monitoring Intracellular Labile Iron Pools: A Novel Fluorescent Iron(III) Sensor as a Potential Non-Invasive Diagnosis Tool. *J. Pharm. Sci.* **2009**, *98*, 2212−2226.
(18) Ma, Y.; Luo, W.; Quinn, P. J.; Liu, Z.; Hider, R. C. Design, Synthesis, Physicochemical Properties, and Evaluation of Novel Iron Chelators with Fluorescent Sensors. *J. Med. Chem.* **2004**, *47*, 6349−6362.
(19) Weizman, H.; Ardon, O.; Mester, B.; Libman, J.; Dwir, O.; Hadar, Y.; Chen, Y.; Shanzer, A. Fluorescently-Labeled Ferrichrome Analogs as Probes for Receptor-Mediated, Microbial Iron Uptake. *J. Am. Chem. Soc.* **1996**, *118*, 12368−12375.
(20) Chen, W.-D.; Gong, W.-T.; Ye, Z.-Q.; Lin, Y.; Ning, G.-L. FRET-Based Ratiometric Fluorescent Probes for Selective Fe^{3+} Sensing and Their Applications in Mitochondria. *Dalton Trans.* **2013**, *42*, 10093−10096.
(21) Lee, M. H.; Giap, T. V.; Kim, S. H.; Lee, Y. H.; Kang, C.; Kim, J. S. A Novel Strategy to Selectively Detect Fe(III) in Aqueous Media Driven by Hydrolysis of a Rhodamine 6G Schiff Base. *Chem. Commun.* **2010**, *46*, 1407−1409.
(22) Wang, B.; Hai, J.; Liu, Z.; Wang, Q.; Yang, Z.; Sun, S. Selective Detection of Iron(III) by Rhodamine-Modified Fe_3O_4 Nanoparticles. *Angew. Chem., Int. Ed.* **2010**, *49*, 4576−4579.
(23) Yang, Z.; She, M.; Yin, B.; Cui, J.; Zhang, Y.; Sun, W.; Li, J.; Shi, Z. Three Rhodamine-Based "Off−On" Chemosensors with High Selectivity and Sensitivity for Fe^{3+} Imaging in Living Cells. *J. Org. Chem.* **2011**, *77*, 1143−1147.
(24) Ast, S.; Schwarze, T.; Müller, H.; Sukhanov, A.; Michaelis, S.; Wegener, J.; Wolfbeis, O. S.; Körzdörfer, T.; Dürkop, A.; Holdt, H.-J. A Highly K^+-Selective Phenylaza-[18]Crown-6-Lariat-Ether-Based Fluoroionophore and Its Application in the Sensing of K^+ Ions with an Optical Sensor Film and in Cells. *Chem.—Eur. J.* **2013**, *19*, 14911−14917.
(25) Li, X.; Gao, X.; Shi, W.; Ma, H. Design Strategies for Water-Soluble Small Molecular Chromogenic and Fluorogenic Probes. *Chem. Rev.* **2014**, *114*, 590−659.
(26) Benesi, H. A.; Hildebrand, J. H. A Spectrophotometric Investigation of the Interaction of Iodine with Aromatic Hydrocarbons. *J. Am. Chem. Soc.* **1949**, *71*, 2703−2707.